Observation of Long-Distance Radial Correlation in Toroidal Plasma Turbulence

S. Inagaki,[1,2] T. Tokuzawa,[3] K. Itoh,[2,3] K. Ida,[2,3] S.-I. Itoh,[1,2] N. Tamura,[3] S. Sakakibara,[3] N. Kasuya,[2,3] A. Fujisawa,[1,2] S. Kubo,[3] T. Shimozuma,[3] T. Ido,[3] S. Nishimura,[3] H. Arakawa,[4] T. Kobayashi,[4] K. Tanaka,[3] Y. Nagayama,[3] K. Kawahata,[3] S. Sudo,[3] H. Yamada,[3] A. Komori,[3] and LHD Experiment Group

[1]*Research Institute for Applied Mechanics, Kyushu University, Fukuoka 816-8580, Japan*
[2]*Itoh Research Center for Plasma Turbulence, Kyushu University, Kasuga 816-8580, Japan*
[3]*National Institute for Fusion Science, Gifu 502-5292, Japan*
[4]*Interdisciplinary Graduate School of Engineering Sciences, Kyushu University, Kasuga 816-8580, Japan*

(Received 9 July 2010; published 7 September 2011)

This Letter presents the discovery of macroscale electron temperature fluctuations with a long radial correlation length comparable to the plasma minor radius in a toroidal plasma. Their spatiotemporal structure is characterized by a low frequency of ~1–3 kHz, ballistic radial propagation, a poloidal or toroidal mode number of $m/n = 1/1$ (or $2/1$), and an amplitude of ~2% at maximum. Nonlinear coupling between the long-range fluctuations and the microscopic fluctuations is identified. A change of the amplitude of the long-range fluctuation is transmitted across the plasma radius at the velocity which is of the order of the drift velocity.

DOI: 10.1103/PhysRevLett.107.115001 PACS numbers: 52.35.Ra, 52.25.Fi, 52.55.Hc

Plasma turbulence has been known as a primary origin of cross-field transport in magnetically confined plasmas [1]. Recently, mesoscale structures, such as zonal flows and streamers, have been found to be nonlinearly generated by microscale fluctuations and to play an important role in determining the turbulent transport [2–5]. The MHD modes can also interact with micro- or macroscale fluctuations and affect transport [6]. Although the study of turbulent transport is in progress, the well-known phenomena ''transient transport events'' remain unexplained [7–12]: A change of local transport occurs very rapidly, in response to a change of plasma parameters at a distant position. The occurrence of such rapid transmission is independent of plasma size, plasma confinement mode, and global MHD stability; that is, this problem is one of fundamental processes in toroidal plasmas. These facts indicate that identification of all the possible fluctuations in confined plasmas remains an urgent issue. In contrast with rich experimental evidence for mesoscale as well as microscale fluctuations, the knowledge of fluctuations, which have very long radial correlation lengths, have been limited except in MHD modes.

In the past, only a few examples of fluctuation measurements on electron temperature T_e have been available [13–15], including several works on MHD-related T_e fluctuations [16–18]. Recently, tens of kHz T_e fluctuations have been observed [19–21]. In Large Helical Device (LHD), a 28-channel electron cyclotron emission (ECE) radiometer has been provided covering an entire plasma minor radius [12,22]. Radial resolution of the radiometer varies from 2.5 cm in the region of $\rho < 0.2$ to 1 cm in the regions of $\rho > 0.4$. The Gaussian-beam waist radius is ~3 cm at each electron cyclotron resonance surface; here ρ is the normalized average radius. By using this ECE radiometer, the low-frequency T_e fluctuations with long-range correlations were found in low-density plasmas. We report the discovery of a new kind of a macroscale fluctuation, the structure of which is three dimensionally determined by several cross-correlation analyses by use of other diagnostics (microwave reflectometer and array of magnetic probes).

The experiments are carried out on the LHD, which has a major radius R of 3.5 m, an averaged minor radius of 0.6 m, and a magnetic field strength on the axis B_{ax} of 2.83 T. The temporal evolution of the typical discharges presented here is shown in Fig. 1(a). The target plasma is produced with neutral beam injection of 2 MW, then at $t = 2.5$ sec electron cyclotron resonant heating (ECRH) of 1 MW is superimposed at the plasma center. During the discharges, the line-averaged density is almost constant at $\bar{n}_e = 0.4 \times 10^{19}$ m^{-3}, and the central T_e is found to increase from 1.5 to 4 keV after the superposition of ECRH. Figure 1(c) shows, for reference, the T_e and n_e profiles at $t = 2.8$ sec, measured with an ECE radiometer and a 13-channel far-infrared interferometer [23], respectively. In the ECRH phase, the volume averaged β is 0.1% and the electron collision frequency normalized by bounce frequency of helical ripple-trapped orbit is ~0.03. The magnetic fluctuations are small, $\tilde{b}/B_{\mathrm{ax}} < 10^{-6}$, at probe position, and tens of kHz fluctuations driven by high-energy particles (e.g., the reversed shear Alfvén eigenmode [24]) are not observed. The plasma has neither a transport barrier nor power modulation.

Correlation analysis is applied during the quiet period from $t = 2.7$ to 2.8 sec, using an ECE radiometer that gives radiation temperature (T_{rad}), with supporting fluctuation measurements with an X-mode reflectometer (RM) [25] and magnetic probes (MAG) [26] [locations of which are

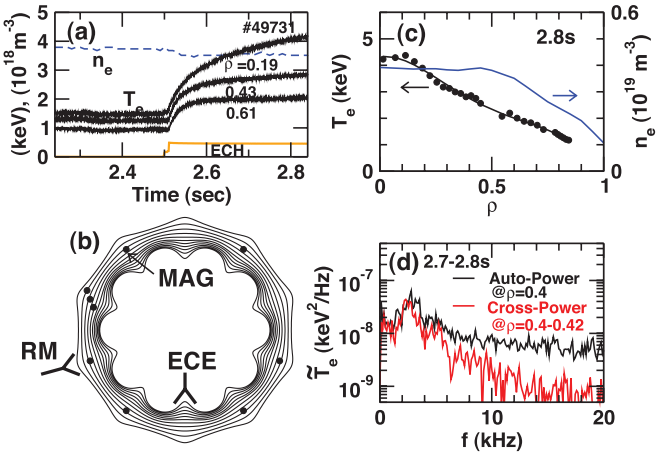

FIG. 1 (color). (a) Typical time evolution of T_e and the line-averaged density. (b) Contour plot of the magnetic flux surfaces on equatorial midplane of LHD. Measurement locations of magnetic probes (MAG) used in this analysis are indicated by filled circles. The reflectometer (RM) antenna and the ECE antenna are located apart from each other by 72° in a toroidal direction. (c) Radial profiles of T_e and n_e at 2.8 sec. (d) Autopower spectrum of $\tilde{T}_{\rm rad}$ at $\rho = 0.4$ and cross-power spectrum between two adjacent channels of $\tilde{T}_{\rm rad}$ at $\rho = 0.4$ and 0.42. The time window for fast-Fourier transform (FFT) is 8 msec and 30 ensembles are averaged.

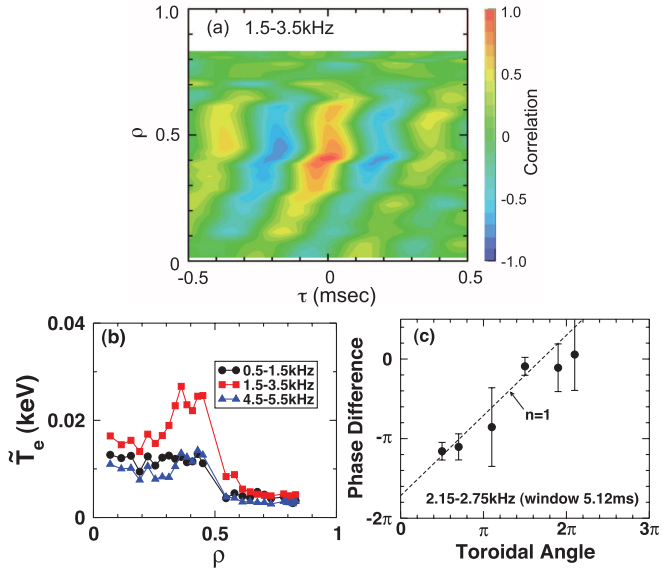

FIG. 2 (color). (a) Contour plot of the cross-correlation function of the low-frequency component (1.5–3.5 kHz) of $\tilde{T}_{\rm rad}$ from 28-ECE channels with that of the reference channel at $\rho = 0.4$. (b) Radial profile of the amplitude of $\tilde{T}_{\rm rad}$ in the three characteristic frequency bands. (c) Cross phase between $\tilde{T}_{\rm rad}$ at $\rho = 0.4$ and the toroidal magnetic probe array. The straight line gives the toroidal mode number $n = 1$.

denoted in Fig. 1(b)]. Figure 1(d) displays the Fourier spectrum of $\tilde{T}_{\rm rad}$ during the ECH phase at $\rho = 0.4$. The possible difference between $T_{\rm rad}$ and T_e is discussed later. The autopower spectrum shows an unambiguous peak around 2.5 kHz with ~1 kHz bandwidth. At higher frequencies ($f > 6$ kHz) the spectrum has a dependence $f^{-1/2}$, corresponding to random noise [18]. The random noise can be suppressed in the cross-power spectrum between two radially adjacent channels. The significant $\tilde{T}_{\rm rad}$ is routinely observed in the low-frequency region.

The spatiotemporal structure of $\tilde{T}_{\rm rad}$ is determined by a two-point two-time correlation at different radii. Figure 2(a) shows a contour plot of correlations of $\tilde{T}_{\rm rad}$ at 28 ECE channels with that of the reference channel at $\rho = 0.4$ (signals are filtered within the bandwidth of 1.5–3.5 kHz). The fluctuations have a long radial correlation, which extends from the center to the peripheral region. The radial wavelength is of the order of the plasma radius. The outward propagation is ballistic, and the radial phase velocity is around 1 km/s, which is of the order of the diamagnetic drift velocity. The radial profile of the fluctuation amplitude is shown in Fig. 2(b), and $\tilde{T}_{\rm rad}$ exceeds 20 eV at $\rho \sim 0.4$. The toroidal and poloidal mode numbers of $\tilde{T}_{\rm rad}$ are measured by cross correlation between signals from ECE and magnetic probes that give a small but finite signal $\tilde{b}/B_{\rm ax} < 10^{-6}$ at the probe position. The cross phase between a 6-channel toroidal array of magnetic probes and an ECE channel (at $\rho = 0.4$) in the frequency range of ~2.5 kHz indicates that the toroidal mode number is $n = 1$ as shown in Fig. 2(c). The cross phase using the 4-channel poloidal array shows the poloidal mode number $m = 1 - 2$ (the fluctuation propagates in the ion diamagnetic direction). The spatiotemporal structure of $\tilde{T}_{\rm rad}$ is unambiguously shown.

The long-range fluctuations are also observed in the signal of the RM, which measures the local density fluctuation $\tilde{n}_e$ at $\rho = 0.40$–0.43. The density fluctuations in the high frequency band (≥ 100 kHz) are modulated by the ambient low-frequency perturbation; therefore, the envelope of it can show the background electric field variation. The modulation effects are predicted in theory and confirmed in experiments [4]. The envelope is calculated by using a Hilbert transform [Fig. 3(a)]. The Fourier spectrum of the envelope, $I_n(t)$, shows that fluctuations ranging from 0.2 to 5 kHz exist in RM signals [Fig. 3(b)]. Significant cross correlation between $I_n(f)$ at $\rho = 0.4$–0.43 and $\tilde{T}_e(f)$ of each ECE channel is demonstrated in the frequency range of 0.2–5 kHz and the wide radial region [Fig. 3(c)]. The variation of the electrostatic potential $\Delta\Phi$ of this long-range fluctuation can be estimated from I_n. The study of disparate-scale interactions has given the estimate $\tilde{I}_n(f)/\langle I_n\rangle \sim f_{\rm micro} f^{-1} k_r L_n (e\Delta\Phi/T_e)$, where $\langle I_n\rangle$ is the mean of the envelope of microscopic fluctuations, $f_{\rm micro}$ is the frequency of micro fluctuations, and f and k_r are the frequency and the radial wave number, respectively, of long-range perturbation [2]. By substituting observed values $\tilde{I}_n/\langle I_n\rangle \sim 0.3$ and $k_r L_n \sim 1$ for $f_{\rm micro} \sim 100$ kHz, one has $e\Delta\Phi/T_e \sim 0.01$. This indicates that $e\Delta\Phi$ is of the same order of magnitude as $\tilde{T}_{\rm rad}$.

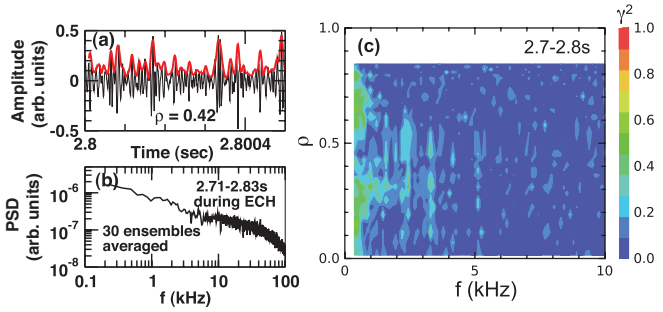

FIG. 3 (color). (a) Typical time evolution of high-pass filtered (≥ 100 kHz) reflectometer signal (black line) and its envelope (red line) during ECH phase. (b) Power spectrum density of the envelope of the reflectometer signal. (c) Contour plot of the squared coherence between the envelope of reflectometer signal and the 28-channel ECE signals in the space of frequency versus radial location of each ECE channel for 2.7–2.8 sec. The time window for FFT is 8 msec and 30 ensembles are averaged.

Auto-bicoherence of each ECE signal shows nonlinear coupling of the long-range $\tilde{T}_{\mathrm{rad}}$ (1.5–3.5 kHz) with their second harmonics. However, it is impossible to observe the significant bicoherence between 1.5–3.5 kHz components and high frequency components of $\tilde{T}_{\mathrm{rad}}$, owing to a large level of noise in the higher frequency region (>6 kHz). Nonlinear interactions between the long-range fluctuations and microscopic fluctuations are identified by cross-bispectral analysis among three modes (1, 2, and 3) satisfying the matching condition ($f_1 + f_2 = f_3$). The quantity of $\tilde{n}_e$ is applied to modes 1 and 2 and $\tilde{T}_{\mathrm{rad}}$ is used for mode 3. Here the 3-channel ECE signals ($\rho = 0.4$, 0.42, 0.45), which have the same phase relation at 1.5–3.5 kHz as shown in Fig. 2(a), are used to increase the number of ensembles. The cross-bicoherence in Fig. 4 shows that $\tilde{T}_{\mathrm{rad}}$ around 2.5 kHz couples nonlinearly with high frequency $\tilde{n}_e$, although no causal relationship between them can be resolved. The fluctuations in T_{rad}, T_e, and n_e are related as $\tilde{T}_{\mathrm{rad}}/T_{\mathrm{rad}} = (1 + C)\tilde{T}_e/T_e + C\tilde{n}_e/n_e$, where $C = \tau/[\exp(\tau) - 1]$ and τ is the optical thickness [27]. In the present experiment, $\tau > 4$ is satisfied in the plasma core, so that the dominant contribution to $\tilde{T}_{\mathrm{rad}}$ comes from $\tilde{T}_e$ (in the edge region, $\tau \sim 1$ holds so that $\tilde{T}_{\mathrm{rad}}$ is influenced by $\tilde{n}_e$ as well). Comparison between the auto-bicoherence of $\tilde{T}_{\mathrm{rad}}$ and $\tilde{n}_e$ also indicates that the contamination of $\tilde{n}_e$ in $\tilde{T}_{\mathrm{rad}}$ is negligible. Thus a working hypothesis that the dominant contribution to $\tilde{T}_{\mathrm{rad}}$ comes from $\tilde{T}_e$ is allowed.

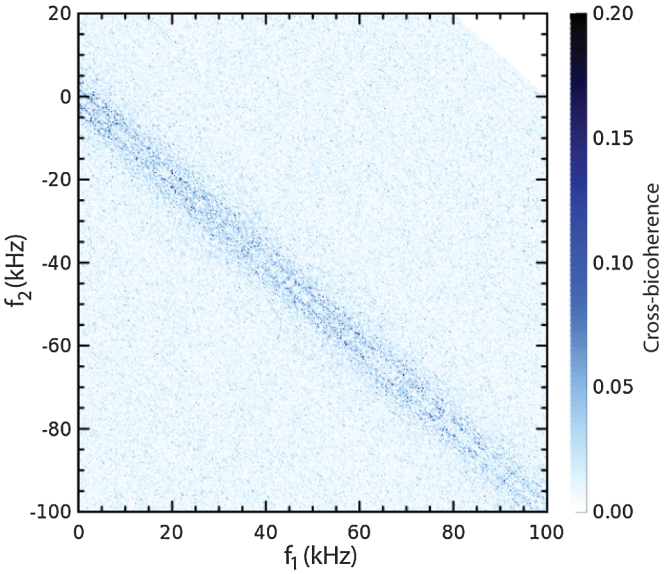

FIG. 4 (color). Contour plot of squared cross-bicoherence between n_e and T_{rad} fluctuations for 2.6–2.8 sec. The time window for FFT is 8 msec and 360 ensembles are averaged.

Figure 5 shows a spontaneous change of the low-frequency fluctuations with long-range structure. The mean temperature decreases slightly after the increase in the fluctuation amplitude, indicating the change of the mean transport. The change of the mode amplitude propagates from core to edge with a time scale of 0.1 msec. That is, the propagation speed of the change of amplitude is ~ 1 km/s.

It is worth discussing the relation with MHD activities such as interchange modes [28]. The MHD perturbation at the presently observed level of $\tilde{b}/B_{\mathrm{ax}} < 10^{-6}$ yields very small deformation of the magnetic surface [less than 0.5 mm at the $m = 2$ resonant surface ($\rho = 0.36$)]. The evaluated magnetic field displacement at resonant surface gives a too small $\tilde{T}_{\mathrm{rad}}$ variation (less than 2.6 eV), which is inconsistent with the observed perturbation (30 eV).

The impact of this long-range fluctuation on transport is analyzed. The radial excursion l of the equicontour of T_{rad} of the observed mode (Fig. 2) is $l \sim 5$ mm, and is much smaller than the wavelength. A random walk model gives an effective diffusion coefficient, $D_{\mathrm{eff}} \sim 0.2$ m^2/s, by

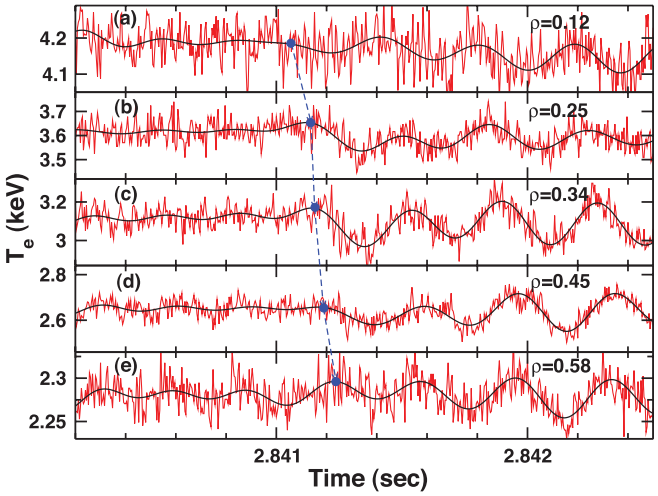

FIG. 5 (color). Typical time evolution of T_{rad} fluctuation (red line) and low-pass filtered (≤ 3.5 kHz) signal (black line) at abrupt change of fluctuation amplitude. The onsets of change of amplitude (blue circles) are evaluated from envelope of low-passed signal measured at each radius.

employing the step size of $l \sim 5$ mm and observed decorrelation rate of 10^4 s^{-1}. This value of $D_{\rm eff}$ is 1/10 of the total electron transport in the stationary state, but the fluctuation can have a substantial role in the dynamical change of transport. Figure 5 indicates that the change of transport (the order of 10^{-1} of mean value) propagates in the radius at a speed that is approximately 100 times faster than that of global energy.

What is common to models of the transient transport event is the view that fluctuations with long radial correlation length can exist in confined plasmas [29–34]. The discovery of this long-range fluctuating structure stimulates the comparison of it with the transient transport event in low-collisionality LHD plasmas. A cold-pulse propagation experiment on LHD has shown that (1) the abrupt change in the heat flux is ~10% of the stationary value, (2) the change propagates with a velocity of 0.4–0.8 km/s in the central region, (3) and significant correlation exists between the change of central heat fluxes and the change of the T_e gradient at $\rho \sim 0.6$ [35]. The newly discovered long-range fluctuations show some similarities to what has been observed in conjunction with transient transport events. Moreover, the observed linkage of the fluctuating structure with local microscale fluctuation (in Fig. 4) implies that local microfluctuations communicate with those at distant radius via this long-range fluctuation. In a previous observation of long-range $\tilde{T}_e$, $n = 0$ is conjectured [15]. Identification of a toroidal or poloidal structure of the long-range $\tilde{T}_{\rm rad}$ is essential.

According to the observed frequency, a possible candidate of this fluctuation is the linearly stable dissipative trapped-ion mode (DTIM) [36]. The relation $|k_\parallel v_{{\rm th},i}| > \omega > \omega_{b,i} > \epsilon^{-1}\nu_i$ is satisfied for the fluctuation of interest ($v_{{\rm th},i}$ and ν_i, ion thermal speed and collision frequency; $k_\parallel$, parallel wave number; $\omega_{b,i}$, bounce frequency of trapped ions; ω, angular frequency of wave; and $\epsilon = r/R$). The dispersion relation was given as $\omega_{\rm DTIM} \simeq (\sqrt{\epsilon}/2)\omega_*$, and $\gamma = \epsilon^2\nu_e^{-1}\omega_*^2/4 - \epsilon^{-1}\nu_i$ [36]. Considering the positive mean electrostatic potential (which is of the order of T_e) [37], a Doppler shift of $\omega_{E\times B} \sim -m \times 10^4$ s^{-1} occurs. Thus, the dispersion relation in the laboratory frame is $\omega_{\rm lab} = \omega_{\rm DTIM} + \omega_{E\times B} \sim -(1 + \sqrt{\epsilon}/2)m \times 10^4$ s^{-1}. The observed frequency is close to $\omega_{\rm lab}$, and the spectral width of excited fluctuations is close to the damping rate γ.

In summary, we have discovered the macroscale and low-frequency electron temperature fluctuations with long-distance correlation coupled with microscopic fluctuation. We have identified the spatiotemporal structure of the long-range fluctuations using correlation techniques based on an ECE measurement with ones of magnetic probes and a reflectometer. Our discovery of long-range fluctuation and its dynamic response give basic insights into the understanding of rapid transmission of change of transport between two distant positions in nonequilibrium inhomogeneous plasmas.

We thank Professor P. H. Diamond, Dr. T. Yamada, Dr. Y. Nagashima, and Professor M. Yagi for useful discussion. We are grateful to the technical group at NIFS for their excellent support. This work is partly supported by a grant-in-aid for scientific research of JSPF, Japan (21224014, 19360148) and by the collaboration programs of NIFS (NIFS07KOAP017, NIFS10KOAP023) and of the RIAM of Kyushu University and Asada Science foundation.

[1] J. A. Wesson, *Tokamaks* (Oxford University Press, Oxford, 1987).
[2] P. H. Diamond *et al.*, Plasma Phys. Controlled Fusion **47**, R35 (2005).
[3] A. Fujisawa *et al.*, Phys. Rev. Lett. **93**, 165002 (2004).
[4] Y. Nagashima *et al.*, Plasma Phys. Controlled Fusion **49**, 1611 (2007).
[5] T. Yamada *et al.*, Nature Phys. **4**, 721 (2008).
[6] W. X. Ding *et al.*, Phys. Rev. Lett. **99**, 055004 (2007).
[7] L. Laurent, Plasma Phys. Controlled Fusion **28**, 85 (1986).
[8] E. D. Fredrickson *et al.*, Phys. Rev. Lett. **65**, 2869 (1990).
[9] J. G. Cordey *et al.*, Plasma Phys. Controlled Fusion **36**, A267 (1994).
[10] K. W. Gentle *et al.*, Phys. Plasmas **2**, 2292 (1995).
[11] U. Stroth *et al.*, Plasma Phys. Controlled Fusion **38**, 1087 (1996).
[12] S. Inagaki *et al.*, Nucl. Fusion **46**, 133 (2006).
[13] S. Sattler, H. J. Hartfuss, and W7-AS Team, Phys. Rev. Lett. **72**, 653 (1994).
[14] C. Watts and R. F. Gandy, Phys. Rev. Lett. **75**, 1759 (1995).
[15] P. A. Politzer, Phys. Rev. Lett. **84**, 1192 (2000).
[16] A. E. Costley, Plasma Phys. Controlled Fusion **30**, 1455 (1988).
[17] H. K. Park *et al.*, Phys. Rev. Lett. **96**, 195003 (2006).
[18] A. Cavallo and R. Cano, Plasma Phys. **23**, 61 (1981).
[19] A. G. Lynn *et al.*, Plasma Phys. Controlled Fusion **46**, A61 (2004).
[20] A. E. White *et al.*, Phys. Plasmas **17**, 020701 (2010).
[21] A. E. White *et al.*, Phys. Plasmas **17**, 056103 (2010).
[22] K. Kawahata *et al.*, Rev. Sci. Instrum. **74**, 1449 (2003).
[23] K. Tanaka *et al.*, Nucl. Fusion **46**, 110 (2006).
[24] K. Toi *et al.*, Phys. Rev. Lett. **105**, 145003 (2010).
[25] T. Tokuzawa *et al.*, Proc. EPS Conf. **31**, P5 (2004).
[26] S. Sakakibara *et al.*, Nucl. Fusion **41**, 1177 (2001).
[27] S. Kubo *et al.*, AIP Conf. Proc. **669**, 187 (2003).
[28] A. Isayama *et al.*, Plasma Phys. Controlled Fusion **48**, L45 (2006).
[29] P. H. Diamond and T. S. Hahm, Phys. Plasmas **2**, 3640 (1995).
[30] X. Garbet *et al.*, Phys. Plasmas **5**, 2836 (1998).
[31] S.-I. Itoh and K. Itoh, Plasma Phys. Controlled Fusion **43**, 1055 (2001).

[32] G. Zaslavsky, *Hamiltonian Chaos and Fractional Dynamics* (Oxford University Press, Oxford, 2005).
[33] T. Iwasaki *et al.*, J. Phys. Soc. Jpn. **68**, 478 (1999).
[34] D. del Castillo-Negrete, AIP Conf. Proc. **1013**, 207 (2008).
[35] S. Inagaki *et al.*, Plasma Phys. Controlled Fusion **52**, 075002 (2010).
[36] B. B. Kadomtsev and O. P. Pogutse, Nucl. Fusion **11**, 67 (1971).
[37] T. Ido *et al.*, Plasma Sci. Technol. **11**, 460 (2009).